

AIRFOIL-SHAPED EXTENSION-TWIST-COUPLED COMPOSITE STAR-BEAMS FOR ROTOR  
BLADE TIP APPLICATIONS

by

STHANU MAHADEV

Presented to the Faculty of the Graduate School of  
The University of Texas at Arlington in Partial Fulfillment  
of the Requirements  
for the Degree of

MASTER OF SCIENCE IN AEROSPACE ENGINEERING

THE UNIVERSITY OF TEXAS AT ARLINGTON

AUGUST 2011

Copyright © by STHANU MAHADEV 2011

All Rights Reserved

## ACKNOWLEDGEMENTS

First and foremost, I would like to thank the great Almighty for his blessings and strength that helped me to initiate and complete my M.S.

I would like to express my fervent and most profound gratitude along with my sincere appreciation to my thesis advisor, Dr. D. Stefan Dancila, for his undivided guidance, constant encouragement, and support, which he has generously provided throughout the preparation of this work. I am indebted to him for many enlightening discussions I had amidst my course of study. I wish to extend my special thanks to Dr. Erian Armanios and Dr. Wen Chan for their willingness to serve on my thesis committee.

I would also like to thank all of my colleagues for their help and support. I would like to especially acknowledge my parents Dr. Vanitha Moorthy and Mr. Sthanu Moorthy and my loving brother Sthanu Mukunda, for their undying understanding, encouragement and love throughout my journey in life.

Thank you. I love you all.

June 28, 2011

## ABSTRACT

### AIRFOIL-SHAPED EXTENSION-TWIST-COUPLED COMPOSITE STAR-BEAMS FOR ROTOR BLADE TIP APPLICATIONS

Sthanu Mahadev M.S

The University of Texas at Arlington, 2011

Supervising Professor: D. Stefan Dancila

Rotorcraft blade tips provide the most effective region for aerodynamic control. Rotor blade airloads are proportional to dynamic pressure and as a consequence are typically the highest in the distal blade tip region. Therefore, blade control using aerodynamic forces and moments is most effectively accomplished over the distal region of the blade. Composite materials represent the preferred material option for modern rotor blade design, especially in the field of rotorcraft and wind energy, due to superior strength-to-weight ratio, fatigue resistance and their ability to be easily tailored to incorporate different coupling (bend-twist, extension-twist, etc.) among elastic modes of deformation within the structure. An additional form of tailoring can produce compliant mechanisms: structures that are capable of producing a deformation such that the resulting displacement field is similar to the kinematics of an actual mechanism. In prior

research, a family of tailored composite structures referred to as “star-beams” and “modified star-beams” have been proposed and investigated as viable candidates for tension-torsion bar applications, including the case of extension-twist coupling, for which “star-beams” preserve the high level of coupling achievable in composite strips. The present work seeks to develop and investigate the extension of prior work to the case of an extension-twist coupled torsionally compliant integral blade tip configuration. The implementation of this structural concept ensures a smooth outer blade-lifting surface and that the smoothness is preserved throughout the desired deformation range while allowing out of plane cross-sectional warping via relative longitudinal sliding along the blade joints. This work focuses on passive control of pitch applications via extension-twist coupling as a result of changes in axial force, typically obtained as a result of change in centrifugal load with rotor speed for a constant thickness, symmetric NACA 0012 airfoil. An ABAQUS based finite element approach is employed to obtain a first characterization of the integral blade tip pitch response to changes in axial load and torque.

## TABLE OF CONTENTS

ACKNOWLEDGEMENTS.....	iii
ABSTRACT.....	iv
LIST OF ILLUSTRATIONS .....	vii
LIST OF TABLES.....	ix
Chapter	Page
1. INTRODUCTION.....	1
1.1 Motivation.....	1
1.1.1 Proposed Integral Blade Tip Configuration .....	2
1.2 Research Objectives .....	3
2. LITERATURE SURVEY .....	4
2.1 Extension-Twist Coupling - A Brief Overview .....	4
2.2 Composite Star-Beams & Modified Star-Beams: Overview.....	5
2.2.1 Basic Concept of Extension-Twist Coupling .....	5
2.2.2 Composite Star-Beams.....	5
2.2.3 Modified Composite Star-Beams .....	7
3. EXTENSION-TWIST COUPLED TORSIONALLY COMPLIANT INTEGRAL BLADE TIP STRUCTURAL CONCEPT COMPUTATIONAL MODELING AND ANALYTICAL FORMULATION .....	9
3.1 Concept of a Compliant Mechanism .....	9
3.2 Problem Statement and Proposed Research Objective .....	9
3.3 Integral Blade-tip Configuration & Computational Modeling .....	10
3.3.1 Integral Blade-tip Computational Model Details.....	12
3.4 Governing Equations to Develop Closed Form Stiffness Equivalent Results .....	15

4. RESULTS AND DISCUSSION .....	18
4.1 Elastomer Stiffness & Ply angle Parametric Study .....	18
4.1.1 Limiting Case-1: Blade Cross Section Excluding Elastomeric Strips.....	19
4.1.2 Limiting Case-2: Blade Cross Section Including Elastomeric Strips with Stiffness = $E_{22}$ of composite .....	21
4.1.3 Case-3: Elastomeric Stiffness= $1/10^{\text{th}} * E_{22}$ of composite .....	23
4.1.4 Case-4: Elastomeric Stiffness= $1/100^{\text{th}} * E_{22}$ of composite .....	26
4.1.5 Case-5: Elastomeric Stiffness= $1/1000^{\text{th}} * E_{22}$ of composite .....	29
4.1.6 Combined Normalized Stiffnesses & Extension-Twist Coupling Plots .....	31
5. CONCLUSIONS AND RECOMMENDATIONS FOR FUTURE WORK .....	34
REFERENCES .....	37
BIOGRAPHICAL INFORMATION.....	39

## LIST OF ILLUSTRATIONS

Figure		Page
1.1	Torsionally compliant integral blade tip: 2-D schematic representation.....	3
2.1	Discretized model of star-beam cross-sectional configuration; $n=4$ .....	6
2.2	Discretized model of deformed star-beam configuration; $n=3$ .....	7
2.3	Modified star-beam: 3-D discretized model .....	8
3.1	Progression from star-beam to torsionally compliant integral blade section.....	12
3.2	Generalized modified star-beam discretized model .....	13
3.3	Elastomeric strip bridged generalized modified star-beam airfoil section .....	14
3.4	6-DOF constrained boundary conditions imposed to mid-section node .....	15
4.1	Normalized axial stiffness (EA) as a function of ply Angle (Case 1).....	20
4.2	Normalized torsional stiffness (GJ) as a function of ply Angle (Case 1).....	20
4.3	Normalized extension-twist coupling (K) as a function of ply angle (Case 1).....	21
4.4	Normalized axial stiffness (EA) as a function of ply Angle (Case 2).....	22
4.5	Normalized torsional stiffness (GJ) as a function of ply angle (Case 2) .....	22
4.6	Normalized extension-twist coupling (K) as a function of ply angle (Case 2).....	23
4.7	Normalized axial stiffness (EA) as a function of ply angle (Case 3) .....	24
4.8	Normalized torsional stiffness (GJ) as a function of ply angle (Case 3) .....	25
4.9	Normalized extension-twist coupling (K) as a function of ply angle (Case 3).....	26



4.10 Normalized axial stiffness (EA) as a function of ply angle (Case 4) .....	27
4.11 Normalized torsional stiffness (GJ) as a function of ply angle (Case 4) .....	28
4.12 Normalized extension-twist coupling (K) as a function of ply angle Case 4) .....	28
4.14 Normalized axial stiffness (EA) as a function of ply angle Case 5) .....	29
4.15 Normalized torsional stiffnesses (GJ) as a function of ply angle (Case 5) .....	30
4.16 Normalized extension-twist coupling (K) as a function of ply angle (Case 5) .....	30
4.17 Combined normalized torsional stiffnesses (EA) as a function of ply angle .....	31
4.18 Combined normalized axial stiffnesses (GJ) as a function of ply angle.....	32
4.19 Combined normalized extension-twist coupling (K) as a function of ply angle .....	32

## LIST OF TABLES

Table	Page
3.1 Material properties (Hexcel IM7/8551-7 Graphite/Epoxy).....	11
3.2 Assumed geometric properties of Integral blade-tip .....	13

## CHAPTER 1

### INTRODUCTION

#### 1.1 Motivation

Numerous applications for composite materials exist and will continue to expand in the aerospace industry due to superior specific mechanical properties such as high stiffness-to-weight ratio, low density characteristics coupled with significant improvements in fatigue resistance compared to their isotropic metal counterparts. In addition, anisotropy makes composite materials desirable for incorporation in primary and secondary structures of fixed wing, rotary wing and wind turbine blade applications. Composite materials can be tailored to generate coupled mechanical behavior within the structure. Mechanical coupling between deformation modes is created by a suitable selection of fiber orientation, stacking sequence, materials and geometric parameters to produce favorable static and dynamic responses.

Elastic tailoring in thin-walled laminated composites provides an extra degree of freedom to meet design requirements more efficiently and economically by reducing part counts. Two outstanding examples of elastically tailored composite laminates are those that exhibit bend-twist and extension-twist coupling. Extension-twist coupling can be achieved in open cross section laminated composites by using an antisymmetric stacking sequence. Extension-twist coupling has application in rotary wing aircraft where an increase in centrifugal load can be used to change the twist distribution in the blade, which in turn can be used to produce a sectional change in the angle of attack of the blade as a function of RPM. Extension-twist coupled blade designs also have potential for use in wind turbines, potentially leading to superior energy output and simpler structural design. Similarly, bend-twist coupling has use in forward swept aircraft wings where an increase in wing loading can produce a wing tip wash-in to prevent tip stall.

Helicopter and windmill rotor blade tips typically provide the most effective region for aerodynamic control. Rotor blade airloads are proportional to dynamic pressure and as a consequence are typically the highest in the distal blade tip region. Additionally, blade tip sections are characterized by large moment arm with respect to the blade root. Control over the blade tip region airloads is also desired because they influence the roll-up formation and development of the blade tip vortex. Therefore, blade control using aerodynamic forces and moments is most effectively accomplished over the distal region of the rotorblade.

Composite materials represent the preferred material option for modern rotor blade design and offer the opportunity to generate compliant mechanisms through an additional form of tailoring. A family of cross sections referred to as “star” and “ modified star” configurations developed and investigated by Dancila, Armanios and Kim [1-4] have proven to represent effective torsionally compliant mechanisms. They were shown to provide tailorable torsional and bending stiffnesses as well as high levels of extension-twist coupling.

#### *1.1.1 Proposed Integral Blade Tip Configuration*

A novel airfoil shaped extension-twist coupled torsionally compliant integral blade tip configuration is proposed, modeled, and investigated that focuses on star-beam type structural concepts for an integral blade tip. It is an innovative outgrowth of the modified star-beam configuration. The integral blade tip configuration is a monolithic, low complexity, passive compliant mechanism concept in which extension-twist coupling is achieved by introducing an antisymmetric composite stacking sequence to the structure.

The implementation of the concept ensures that a smooth outer blade surface is generated for the undeformed configuration and preserved throughout the deformation range while allowing for relative longitudinal displacement along the blade joints thereby allowing the necessary out-of-plane warping of the cross-section that is typical of open cross-sections and an essential requirement for torsional compliance. This is accomplished by bridging the airfoil

upper and lower surface gaps with flexible, linearly elastic, uniform thickness elastomeric (rubber type) strips. The integral blade tip is developed from a NACA 0012 symmetric airfoil (Figure 1.1). Plain stress conditions are assumed for this thin walled, slender structure. An ABAQUS based finite element analysis (FEA) approach is used to model and characterize the mechanical response of this torsionally compliant blade when subjected to a concentrated tip axial force and torque, respectively.

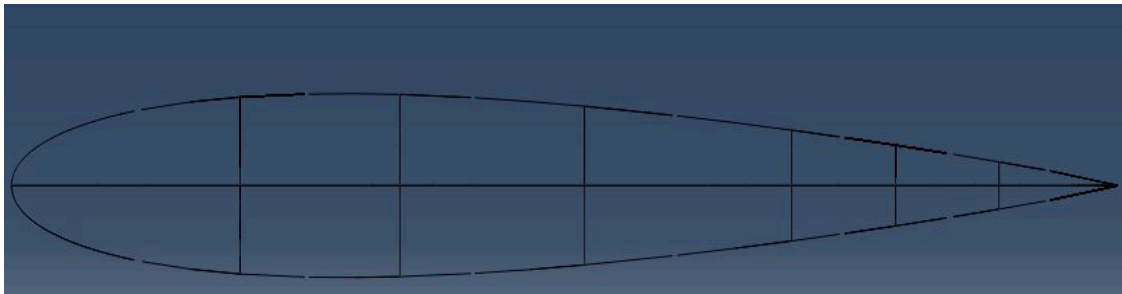


Figure 1.1 Torsionally compliant integral blade tip: 2-D schematic representation

## 1.2 Research Objectives

The present work investigates the influence of elastomeric strip stiffness and composite material ply angle on the axial stiffness, torsional stiffness and the amount of extension-twist coupling achieved. In the present work we are focused on passive control of pitch applications via extension-twist coupling as a result of changes in axial force, typically generated as a result of centrifugal load change with RPM. The current work also takes an initial step in demonstrating the proposed novel torsionally compliant integral blade-tip configuration to be a viable candidate in bridging the gap between a closed cross section and an open cross section.

## CHAPTER 2

### LITERATURE SURVEY

In recent years composite materials have played an increasingly significant role in structural applications. The anisotropy in composite materials provides opportunity to generate additional degrees of freedom thus tailoring elastic properties to induce mechanical deformation modes that results in superior structural performance. For example, extension-twist coupling is of particular relevance due to the high sensitivity of airloads to changes in airfoil angle of attack. Fundamentally this work also focuses on understanding the effect of extension-twist coupling and generation of an effective and efficient methodology to utilize the benefits of the same. The following survey examines previous relevant investigations leading to the conceptualization of a hybrid closed cross section with torsional compliance.

#### 2.1 Extension-Twist Coupling – A Brief Overview

Extension-twist coupling in composite material beams has been investigated for closed and open cross sections. The mechanism that produces extension-twist in thin walled beams is local extension-shear coupling in the wall material due to anisotropy. A key consideration for implementing an elastically tailored mechanism on a structure is to precisely define the relationships between material properties, stacking sequence and cross sectional geometry.

Although closed cell cross-sectional configurations demonstrate high torsional stiffness, the level of extension-twist coupling that can be achieved is substantially lower compared to that of open cross-sectional configurations. However, due to reduced torsional and bending stiffnesses, flat extension-twist coupled strips are of limited usefulness as tailored structural components.

## 2.2 Composite Star-Beams & Modified Star-Beams: Overview

### *2.2.1 Basic Concept of Extension-Twist Coupling*

Extension-twist coupled designs are achieved in laminated composites with open and closed cross sections using anti-symmetric and circumferentially uniform layups, respectively. The fundamental mechanism producing extension-twist coupling is the result of the in-plane extension-shear coupling associated with off-axis plies. In open cross sections such as rectangular flat strips of two lamina subjected to perfect bonding, extension-twist coupling can be produced by stacking a set of unidirectional plies in a  $[\theta_m / -\theta_m]$  angle ply construction. The influence of the in-plane extension shearing action on each half of the laminate is equivalent to that of a pair of opposing forces at each end of the laminate, effectively producing twisting moments. As a result a twisting deformation is produced. Closed cell cross- sections having circumferentially uniform layups exhibits extension-twist coupling as a result of the continuity of shear flow associated with in-plane extension-shear.

### *2.2.2 Composite Star-Beams*

A family of extension-twist coupled star-shape cross-sectional configurations were proposed and analyzed by Dancila, Armanios and Kim [1-4]. These composite beams are characterized by increased torsional and bending stiffness compared to flat strips but maintaining the same level of extension-twist coupling. The need for a beam-type configuration characterized by a level of extension-twist coupling similar to that of flat strips but with bending and torsional stiffnesses significantly increased for implementation of extension-twist coupling in practical rotorcraft applications led to the development of a family of cross sections referred as star-beams.

These configurations were proven analytically, through FEM analysis and experimentally to be a viable solution that preserved the large extension-twist coupling of flat strips with higher bending and torsional stiffnesses compared to flat strips. Several composite star-beam configurations were manufactured and tested to provide an experimental verification of the

analytical model prediction and finite element analysis and was found that the analytical predictions, the finite element analysis and the experimental results were all in good agreement.

The star-beam geometry was considered as an innovative outgrowth of extension-twist coupled flat strips, obtained by joining “n” extension-twist coupled flat substrips, where  $n \geq 2$ , positioned at an equal angle spacing of  $\frac{2\pi}{n}$  around a common central edge (Figure 2.1) for  $n=4$ .

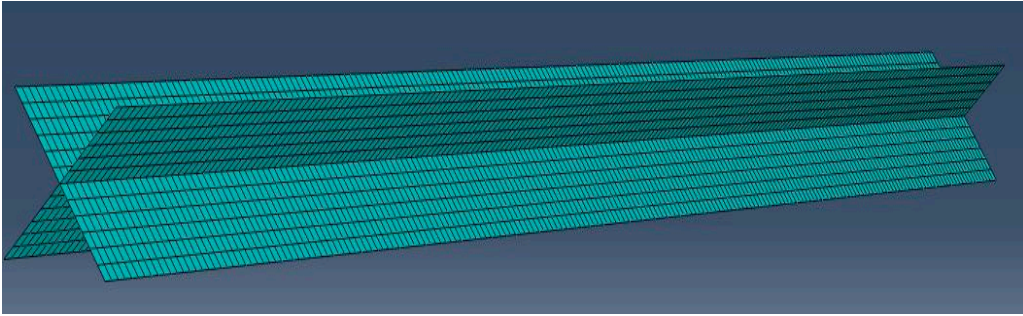


Figure 2.1 Discretized FEM model of star-beam cross-sectional configuration;  $n=4$

The torsional stiffness of the star configuration was also investigated [1]. A comparison study of torsional stiffness values obtained through analytical predictions and experimental analysis was also performed. The results showed good agreement between them and confirmed that the star configuration preserved the level of extension-twist coupling of flat strips while the bending and torsional stiffness were significantly superior [1,2]. A deformed extension-twist coupled beam configuration corresponding to  $n=3$  under axial end force and cantilevered boundary conditions imposed at the other end is shown in Figure 2.2.



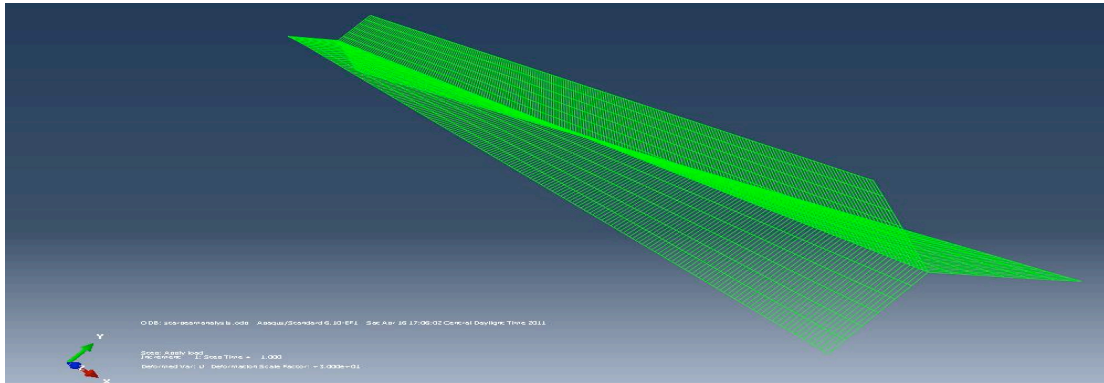


Figure 2.2 Discretized model of deformed extension-twist coupled star-beam configuration;  $n=3$

### 2.2.3 Modified Composite Star-Beams

An extension of the star configuration, the “modified star configuration” [4] was proposed and analyzed by Dancila and Kim [4]. This configuration was obtained from the star configuration by the addition of circular arcs to either side of the substrip (Figure 2.3). It was assumed that the side arcs and the substrip were of the same thickness. These cross-sectional configurations were conceptually considered as a redistribution of a circular cross-sectional area that improved composite tension-torsion frictionless hinge bars. Fundamentally the concept of modified star-beam was proven to be a viable solution to decrease torsional stiffness while increasing bending stiffness.

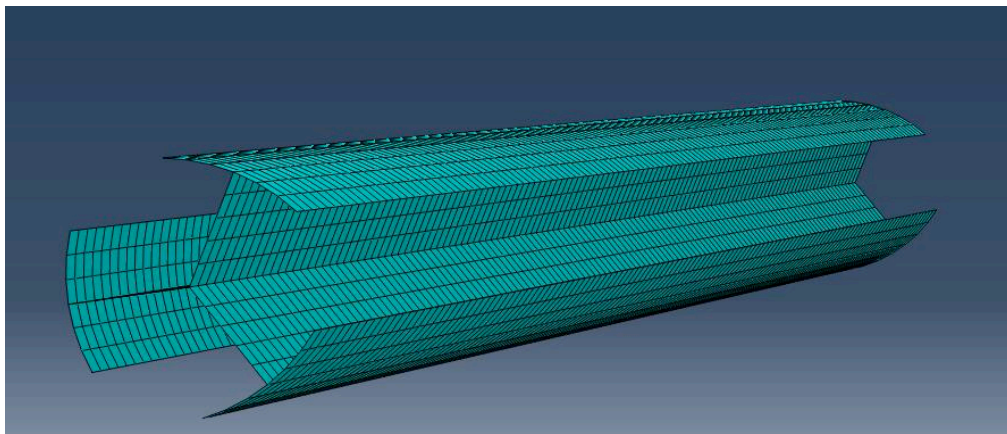


Figure. 2.3 Modified star-beam: 3-D discretized model

It was shown that torsional stiffness can be reduced to less than 7% while the bending stiffness can be increased to more than seven fold and the axial stiffness is still preserved [4]. Modified star-beam cross-sectional configurations were proposed to be effective tension-torsion bar compliant mechanisms for helicopter rotor blade applications. Fundamentally the redistribution of cross-sectional area decreased the torsional stiffness, increased bending stiffness while preserving the level of axial stiffness [4].

Subsequent chapters of this thesis are organized as follows. Chapter 3 will present the configuration and computational modeling for the torsionally compliant integral blade tip configuration. The parametric study showing the influence of elastomer stiffness and ply angle on different stiffnesses is shown in Chapter 4. Chapter 5 discusses the conclusions and recommendations for future work, respectively.

CHAPTER 3  
EXTENSION-TWIST COUPLED TORSIONALLY COMPLIANT INTEGRAL BLADE TIP  
STRUCTURAL CONCEPT  
COMPUTATIONAL MODELING AND ANALYTICAL FORMULATION

3.1 Concept of a Compliant Mechanism

A structure acts as a compliant mechanism if it is capable of producing a deformation such that the resulting displacement field is similar to the kinematics of a mechanism counterpart. Compliant mechanisms are continuous, monolithic parts, thereby eliminating the complexity involved in conventional mechanisms. They also offer the benefit of a frictionless/stictionless operation and reduced part count compared to conventional mechanisms. Star-beams and modified star-beams represent quintessential examples as enhanced composite beam cross-sectional configurations with tension-torsion compliant mechanisms for the elastic support of a helicopter blade tip or a helicopter blade flap.

3.2 Problem Statement and Proposed Research Objective

Based on the literature survey provided in Chapter 2, an integral, torsionally compliant blade tip configuration could offer the dual benefit of tailoring the torsional stiffness and amount of extension–twist coupling while preserving the same level of axial stiffness in practical rotorcraft and wind turbine blade applications.

A novel extension-twist coupled torsionally compliant integral blade tip configuration is proposed and modeled in this work. This includes the development and investigation of an effective integral blade tip that capitalizes and expands upon the previous work on extension-twist coupled star shape composite beams (Figure 3.1). Specifically, it focuses on developing star-beam type structural concepts for the entire blade tip to combine pitch deformation and torsional compliance. Basically the integral blade tip is an outgrowth of the modified star-beam configuration and closes the modified star configuration developed earlier with flexible, uniform thickness, linearly elastic elastomeric strips distributed along the airfoil surface.

### 3.3 Integral Blade -Tip Configuration & Computational Modeling

An ABAQUS based linear FEA approach has been used to model the integral blade tip and to establish the influence of elastomeric strips on the level of extension-twist coupling. The bridging of the small gaps of the cross section with elastomeric strips results in a fundamental change from an open to a closed cross section, which is characterized by higher torsional stiffness and much lower levels of extension-twist coupling. An extension-twist coupled eight ply  $[\theta_4 / -\theta_4]$  antisymmetric lay-up with ply angle " $\theta$ " varying from  $0^\circ$  to  $90^\circ$  is assumed throughout and its influence upon axial stiffness, torsional stiffness and the level of extension-twist coupling are investigated.

Given the focus of this initial work on investigating the effect of variation of elastomeric stiffness, it is assumed that the entire cross section is of uniform thickness including the elastomeric strips. The bi-material integral blade tip is characterized by assuming the composite material properties of Hexcel IM7/8551-7 Graphite/Epoxy as given in Table 3.1[1].

The elastomeric strip is assumed to have a Poisson's ratio of 0.5 and an elastic modulus of 0.1 (Case 3), 0.01 (Case 4), 0.001(Case 5) of the graphite/epoxy transverse axial stiffness, respectively.

Table 3.1 Material properties (Hexcel IM7/8551-7 Graphite/Epoxy)

Parameters	Value
$E_{11}$	146.14 GPa
$E_{22}$	8.472 GPa
$G_{12} = G_{13}$	3.879 GPa
$G_{23}$	3.3 GPa
$\nu_{12} = \nu_{13}$	0.341
$\nu_{23}$	0.5

A uniform integral blade section is modeled and developed computationally in ABAQUS.. A geometrically linear analysis is conducted in this work. Mechanical response of the blade tip is assessed by plotting axial stiffness (EA), torsional stiffness (GJ), and extension-twist coupling (K) term as a function of elastomeric stiffness and ply angle.

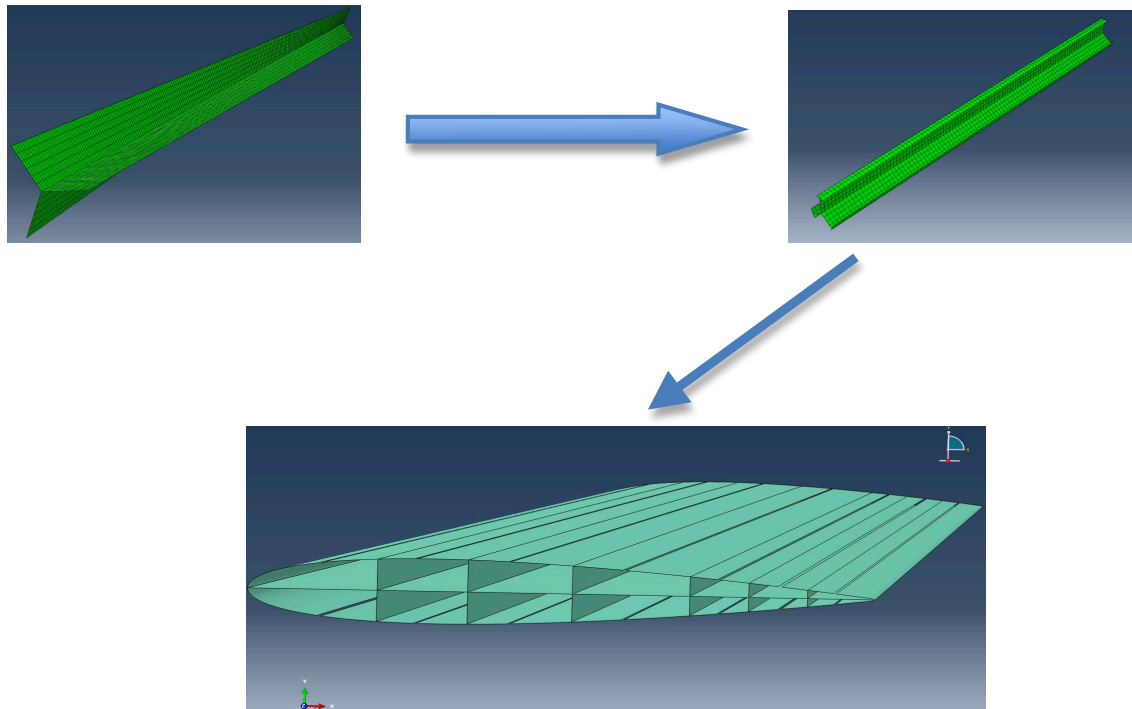


Figure 3.1 Progression from star-beam to torsionally compliant integral blade section

### 3.3.1 Integral Blade-Tip Computational Model Details

For this first investigation of the concept of the NACA 0012 airfoil blade section, a constant chord, uniform cross section with slenderness ratio of 20 is assumed. A 1 m constant chord “ $c$ ” and six webs located at 0.21  $c$ , 0.35  $c$ , 0.52  $c$ , 0.7  $c$ , 0.8  $c$ , 0.89  $c$  from the leading edge form the bi-material support structure for the outer surface skin strips. The width of the elastomeric strips is 0.004 m. The integral blade tip is discretized using S4R quadrilateral reduced integration shell elements and the model size is on the order of 90k elements. Figure 3.2 shows the level of mesh refinement at one end of the discretized structure, with built-in boundary conditions imposed. Table 3.2 shows the geometric characteristics associated with modeling the blade section.

Table 3.2 Assumed geometric properties of integral blade section

Component	Value
Length	20 m
Cross sectional wall midline length	3.40414 m
Ply thickness	138.75 $\mu\text{m}$
Number of plies	8
Laminate thickness	1110 $\mu\text{m}$
Elastomer thickness	1110 $\mu\text{m}$

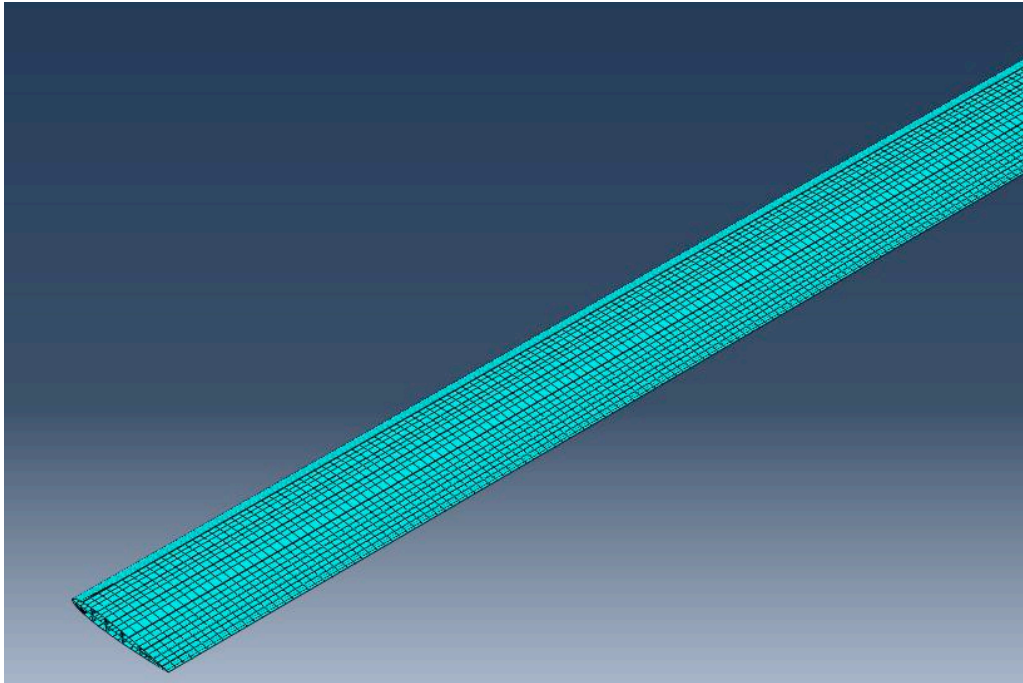


Figure 3.2 Generalized modified star-beam discretized model

The rubber strips are interacted with the blade tip contour by tying the edge nodes of elastomeric strips with the blade tip top and bottom flanges as shown in Figure 3.2.

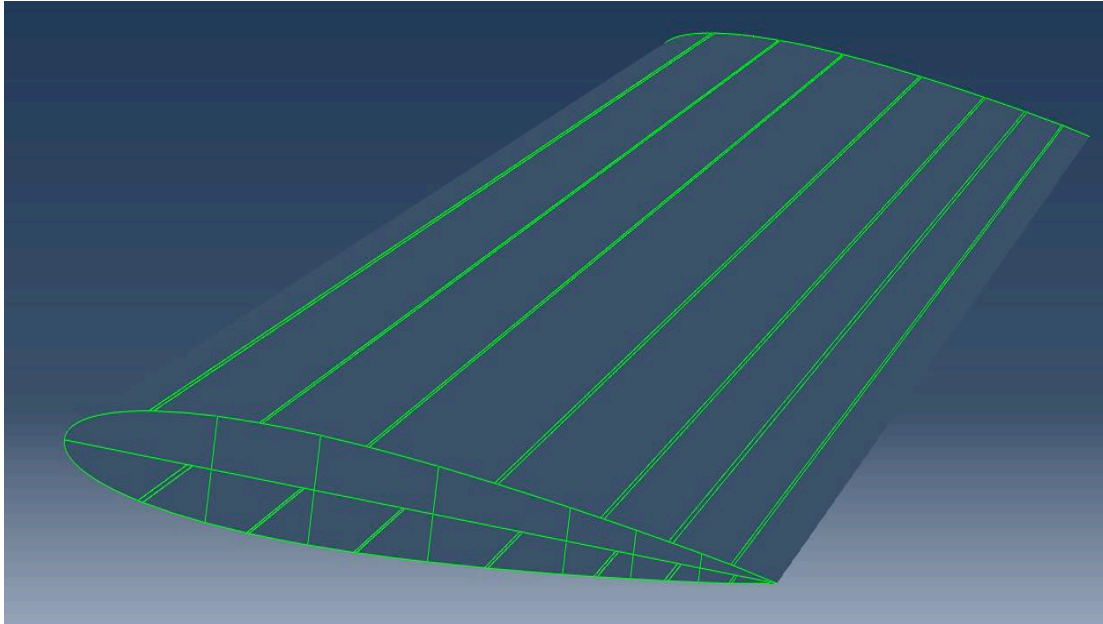


Figure 3.3 Elastomeric strip bridged generalized modified star-beam airfoil section

One node is considered in the mid section of this FEM model with all six degrees of freedom restricted. Both ends of the blade tip section are free to allow for out-of-plane warping, which is an essential requirement for torsional deformation. Equal and symmetric loading is applied at the centroid of the blade tip cross-section to eliminate any effects due to in-plane bending respectively (Figure 3.4). To determine the twist rate ( $\phi'$ ) and the axial displacement rate ( $u'$ ), rotation about the longitudinal axis of the blade tip and the axial displacements along the longitudinal axis of the blade are determined. In order to reduce the influence of end effects two cross-sections located at 40% and 60% (7.911 m, 11.963 m) from the free end of the blade are used to measure relative displacement and rotation. Based upon the relative displacement and rotation of these cross sections and the known distance between them, the corresponding twist



and axial displacement rates have been computed. As a result the axial stiffness (EA), torsional stiffness (GJ), and level of extension-twist coupling (K) are numerically determined.

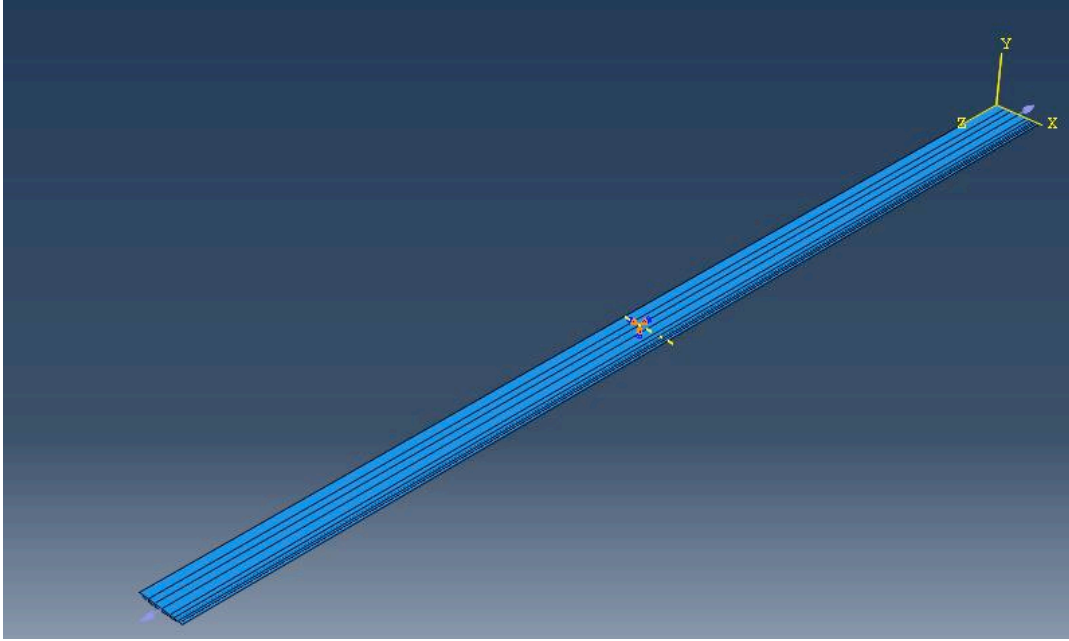


Figure 3.4 6-DOF constrained boundary conditions imposed to mid-section node

### 3.4 Governing Equations to Develop Closed Form Stiffness Equivalent Results

Considering  $N$  to be the applied resultant tip axial force and  $T$  to be the applied resultant tip torque respectively, the corresponding axial displacement rate and twist rate are denoted by  $u'_n, \phi'_n, u'_t, \phi'_t$ . Stiffness equivalents (EA), (GJ) and the level of extension-twist coupling (K) can be generated by relating the above mentioned variables through the following set of linear equations.

The applied axial force  $N$  is related to  $u'_n$  and  $\phi'_n$  according to:

$$N = (EA)u'_n + (K)\phi'_n \quad [3.1]$$

The resultant tip force due to applied torque is zero and is related to  $u_t'$  and  $\phi_t'$  by

$$0 = (EA)u_t' + (K)\phi_t' \quad [3.2]$$

The resultant tip torque due to applied axial force is zero and is related to  $u_n'$  and  $\phi_n'$  by

$$0 = (K)u_n' + (GJ)\phi_n' \quad [3.3]$$

The applied tip torque  $T$  is related to  $u_t'$  and  $\phi_t'$  according to

$$T = (K)u_t' + (GJ)\phi_t' \quad [3.4]$$

These simultaneous equations can be expressed in matrix form as a  $4 \times 3$  system of equations, which needs to be solved for the respective stiffness and coupling terms. The axial stiffness equivalent can be computed as

$$(EA)_{\text{actual}} = \frac{T\phi_n' - \phi_n'u_t'}{\phi_t'u_n' - \phi_n'u_t'} + \frac{N(\phi_t'u_n' - \phi_n'u_t')}{\phi_t'u_n' - \phi_n'u_t'} \quad [3.5]$$

The torsional stiffness equivalent is given by

$$(GJ)_{\text{actual}} = \frac{Tu_n' - \phi_n'u_t'}{\phi_t'u_n' - \phi_n'u_t'} \quad [3.6]$$

The extension-twist coupling equivalent is given by

$$(K)_{\text{actual}} = - \left( \frac{T \phi'_n u'_n}{(-u'_n u'_n \phi'_t - \phi'_n u'_n u'_t)} \right) \quad [3.7]$$

Alternately, the extension-twist coupling term (K) can be assumed to have two distinct values, denoted by  $K_u$  and  $K_\phi$  (Eqns. 3.8 - 3.9), with the expectation that the solution confirms

$K_\phi = K_u$ . The above linear equations can be rewritten as

$$\begin{Bmatrix} N \\ 0 \end{Bmatrix} = \begin{pmatrix} (EA) & (K_\phi) \\ (K_u) & (GJ) \end{pmatrix} * \begin{Bmatrix} u'_n \\ \phi'_n \end{Bmatrix} \quad [3.8]$$

$$\begin{Bmatrix} 0 \\ T \end{Bmatrix} = \begin{pmatrix} (EA) & (K_\phi) \\ (K_u) & (GJ) \end{pmatrix} * \begin{Bmatrix} u'_n \\ \phi'_t \end{Bmatrix} \quad [3.9]$$

Solving these simultaneous equations for axial stiffness, torsional stiffness and two components of extension-twist coupling systematically confirms that the two components of extension-twist coupling are indeed equal and the radius of (EA), (GJ) and (K) in each case match the values obtained by using Eqns. 3.5-3.7.

## CHAPTER 4

### RESULTS AND DISCUSSION

#### 4.1 Elastomeric Stiffness and Ply Angle Parametric Study

We investigate the variation of axial stiffness, torsional stiffness and extension-twist coupling with ply angle “ $\theta$ ” for each of the cases when the elastomeric stiffness is 0.1, 0.01, and 0.001 of the graphite/epoxy transverse axial stiffness, respectively. A combined plot of axial stiffnesses, torsional stiffnesses and the extension-twist coupling as a function of ply angle “ $\theta$ ” is also shown.

The stiffness values are normalized with respect to those of a reference open cross-sectional blade tip configuration without elastomeric strips with a stacking sequence such that  $\theta = 0$ . The reference axial stiffness is given by

$$(EA)_{\text{ref}} = E_{11}bt \quad [3.10]$$

where  $b$  is the cross-sectional wall midline length and  $t$  is the thickness of the wall. The reference torsional stiffness in this case according to the thin walled beam theory is given by

$$(GJ)_{\text{ref}} = \frac{1}{3} G_{12}bt^3 \quad [3.11]$$

The reference value for  $(K)$  is then taken as:

$$(K)_{\text{ref}} = \sqrt{(EA)_{\text{ref}} * (GJ)_{\text{ref}}} \quad [3.12]$$

The equations for obtaining normalized values of axial stiffness, level of extension-twist coupling and torsional stiffness are given by

$$(EA)_{\text{normalized}} = \frac{(EA)_{\text{actual}}}{(EA)_{\text{reference}}} \quad [3.13]$$

$$(GJ)_{\text{normalized}} = \frac{(GJ)_{\text{actual}}}{(GJ)_{\text{reference}}} \quad [3.14]$$

$$(K)_{\text{normalized}} = \frac{(K)_{\text{actual}}}{(K)_{\text{reference}}} \quad [3.15]$$

The numerical values of the reference terms are

$$(EA)_{\text{reference}} = 552.203966 * 10^6 \text{ N}$$

$$(GJ)_{\text{reference}} = 5.981179148 \text{ Nm}^2$$

$$(K)_{\text{reference}} = 57470.26054 \text{ Nm}$$

Two parameters are considered for the study, namely i) ply angle varied from  $0^\circ$  to  $90^\circ$  in steps of  $5^\circ$ , and ii) elastomeric material with an elastic modulus of 0.1, 0.01, and 0.001 of the graphite/epoxy transverse stiffness, respectively while assuming a Poisson's ratio of 0.5. The resulting plots show the effect of these parameters on the mechanical response of the integral blade tip structure.

#### 4.1.1 Limiting Case-1: Blade Cross Section Excluding the Elastomer Strips

In this case, the mechanical response of the integral blade structure is investigated, consisting of only the composite lay-up without the elastomeric strips as a thin walled open cross section slender beam type configuration. The slenderness ratio of this structure is 20. The stiffness plots for axial stiffness (EA), torsional stiffness (GJ) and level of extension-twist coupling are shown in (Figure 4.1- Figure 4.3) respectively.

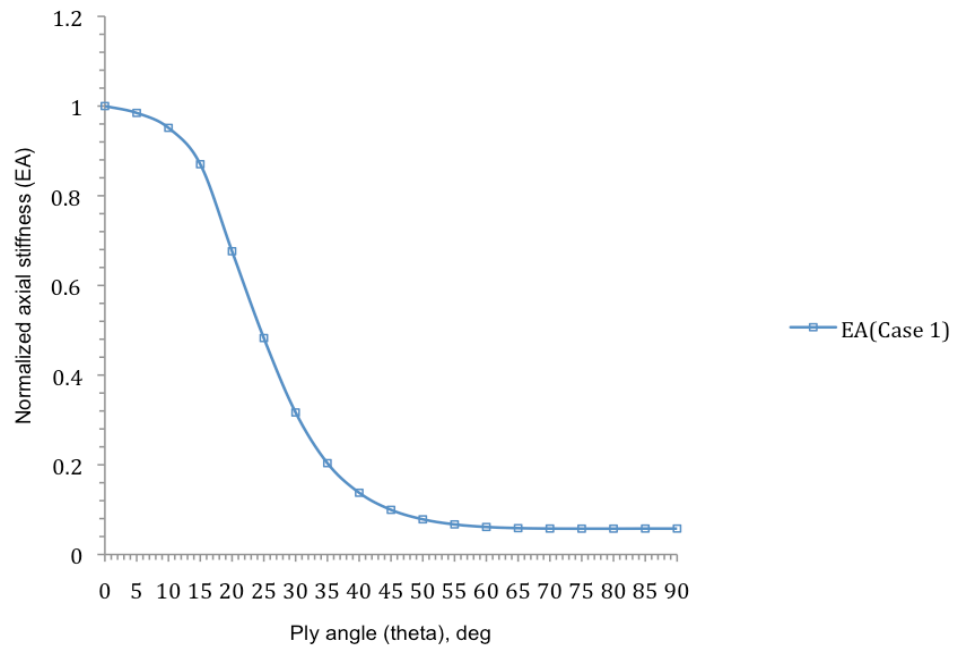


Figure 4.1 Normalized axial stiffness (EA) as a function of ply angle (Case 1)

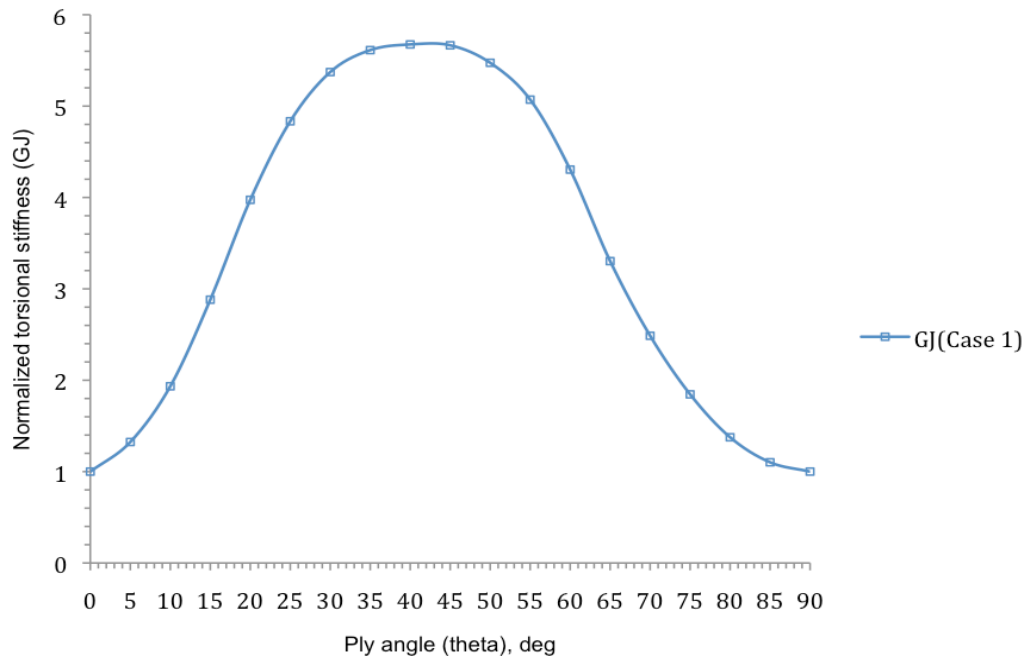


Figure 4.2 Normalized torsional stiffness (GJ) as a function of ply angle (Case 1)

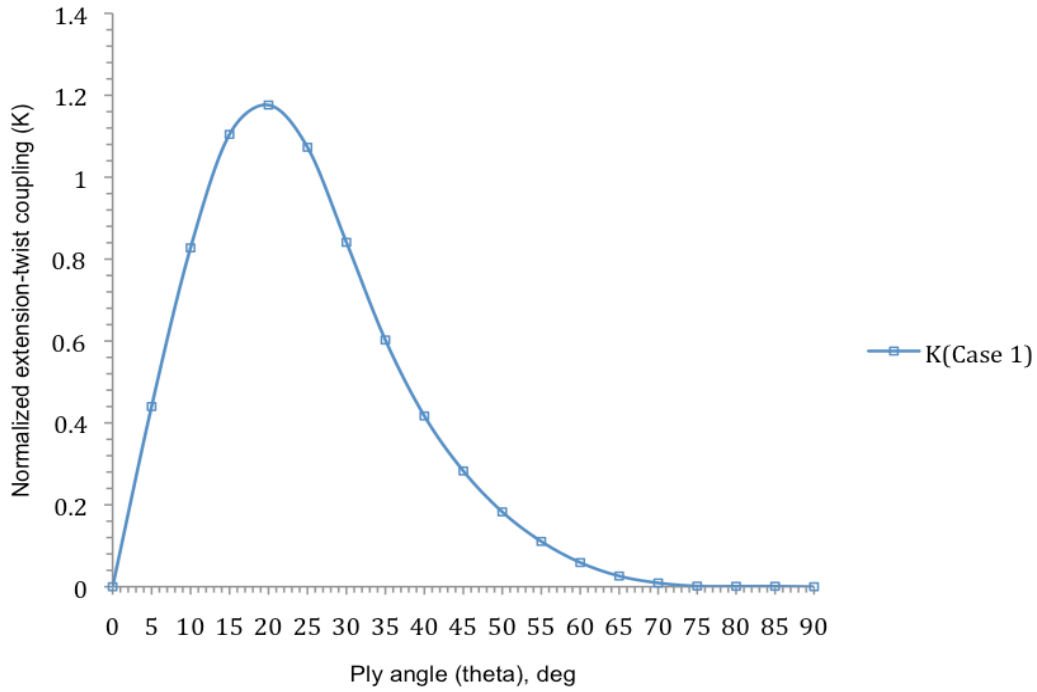


Figure 4.3 Normalized extension-twist coupling (K) as a function of ply angle (Case 1)

#### 4.1.2 Limiting Case-2: Blade Cross Section Including Elastomer Strips with Stiffness= $E_{22}$ of Composite

The integral blade structure attains a closed cell configuration by bridging the airfoil surface gaps with flexible rubber type elastomeric strips. For this limiting case, the elastomeric stiffness is assumed to have an elastic modulus equal to the transverse stiffness of the composite laminate. As expected, this particular configuration generates the highest level of torsional stiffness and provides the least amount of extension-twist coupling (Figure 4.4 – Figure 4.6) without any significant sacrifice in the level of axial stiffness.

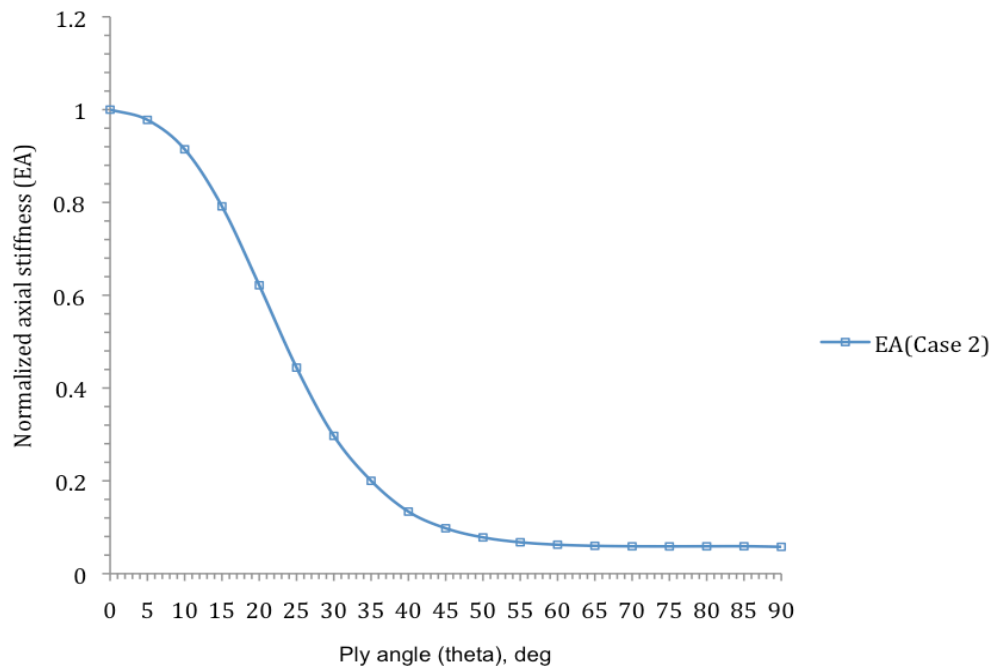


Figure 4.4 Normalized axial stiffness (EA) as a function of ply angle (Case 2)

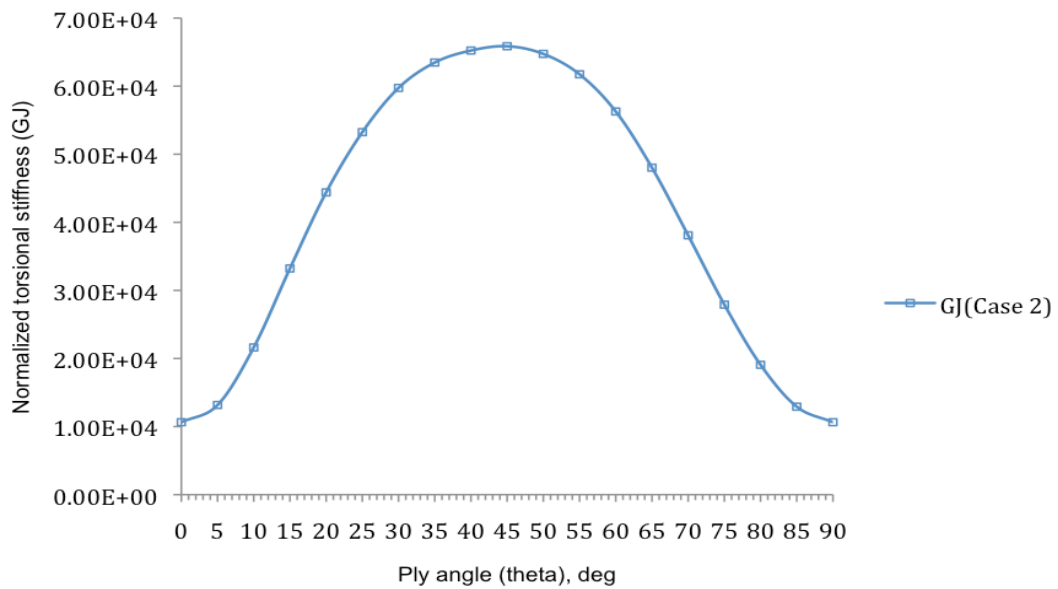


Figure 4.5 Normalized torsional stiffness (GJ) as a function of ply angle (Case 2)



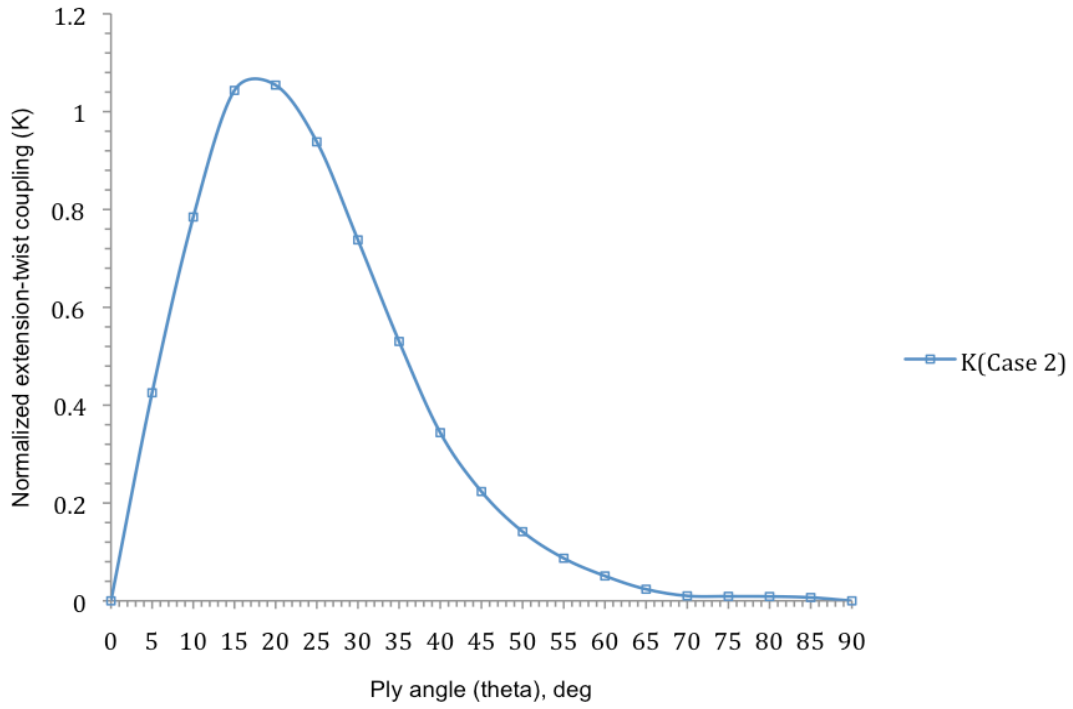


Figure 4.6 Normalized extension-twist coupling (K) as a function of ply angle (Case 2)

#### 4.1.3 Case-3: $E_{22} = 1/10^{th} \text{ of Composite}$

In this case, elastomeric stiffness is lowered by one order of magnitude compared to the transverse modulus of the composite material and assigned a value of 847.2 MPa. The ply angle of the extension-twist coupled eight ply anti-symmetric graphite/epoxy lay-up is varied from  $0^\circ$  to  $90^\circ$  in steps of  $5^\circ$ . Figure 4.7 shows the variation of axial stiffness as a function of ply angle. Maximum axial stiffness is reached for a  $0^\circ$  lay-up and has a value of with the minimum value reached for a  $90^\circ$  lay-up.

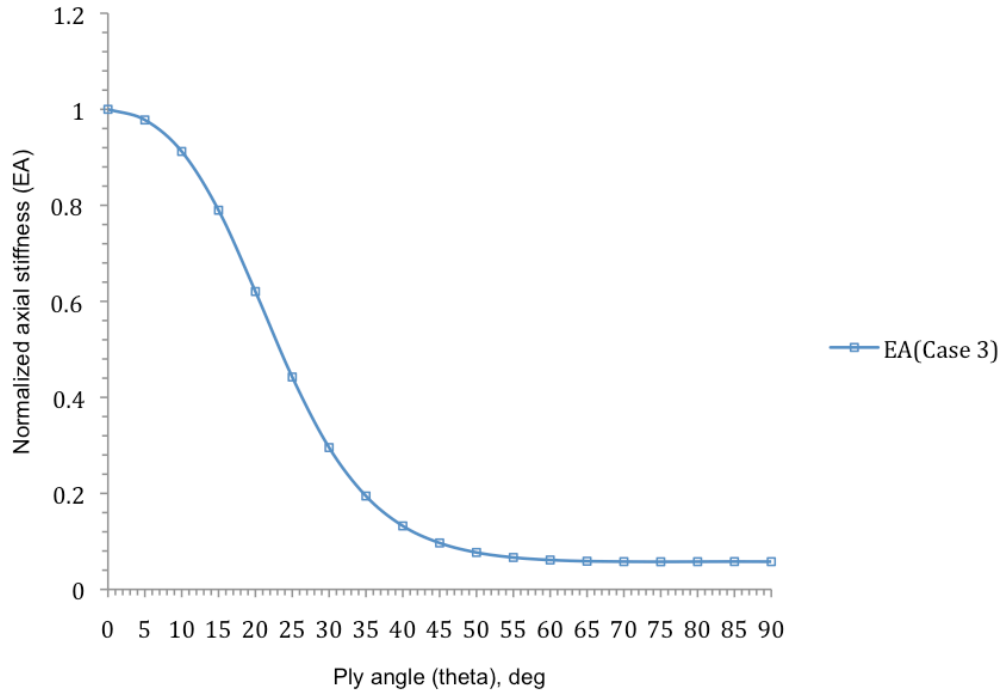


Figure 4.7 Normalized axial stiffness (EA) as a function of ply angle (Case 3)

Normalized torsional stiffness values (Figure 4.8) corresponding to  $0^\circ$  and  $90^\circ$  composite lay-up are  $7.974 \times 10^3$  and  $7.974 \times 10^3$ , thus confirming the author's expectation that the level of torsional stiffness is uniform for these two composite lay-ups. Maximum normalized torsional stiffness is attainable for a  $45^\circ$  composite ply layout with a value of  $20.148 \times 10^3$ . Fundamentally the mechanical response of torsional stiffness with a step increase in ply angle corresponds to the change in the term  $Q_{66}$  of the reduced stiffness matrix derived from classical composite lamination theory.

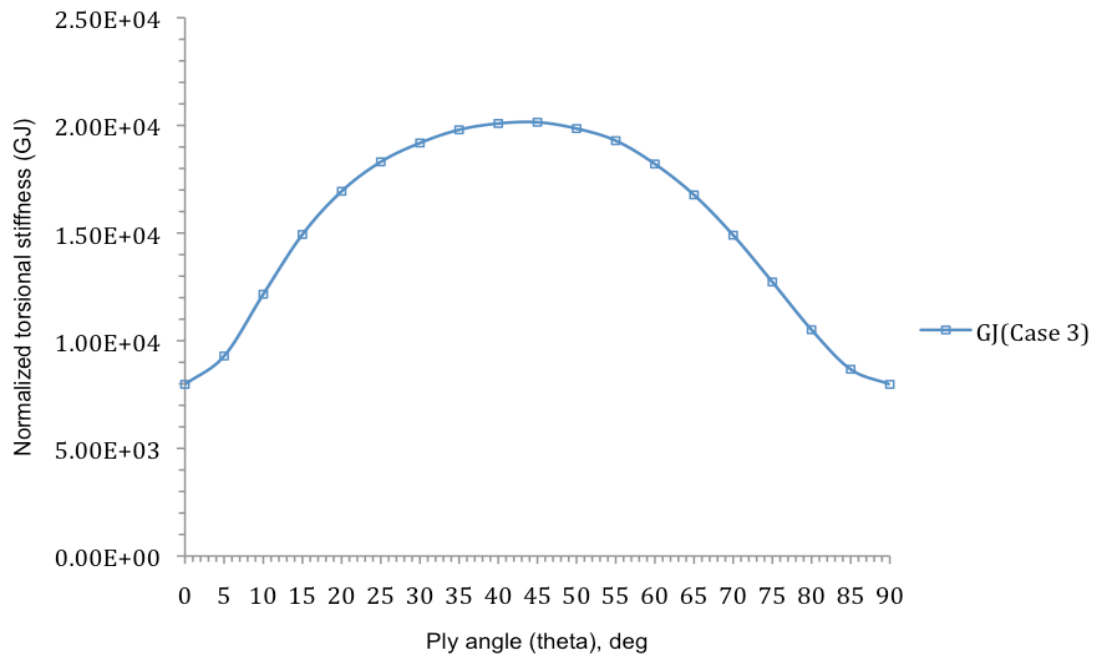


Figure 4.8 Normalized torsional stiffness (GJ) as a function of ply angle (Case 3)

The level of extension-twist coupling as a function of ply angle is shown in Figure 4.9. The effect of coupling is zero for  $0^\circ$  and  $90^\circ$  composite lay-up. Fundamentally the mechanical response of extension-twist coupling for a step increase in ply angle relies on the variation in  $Q_{16}$  term of the reduced stiffness matrix derived from classical composite lamination theory.

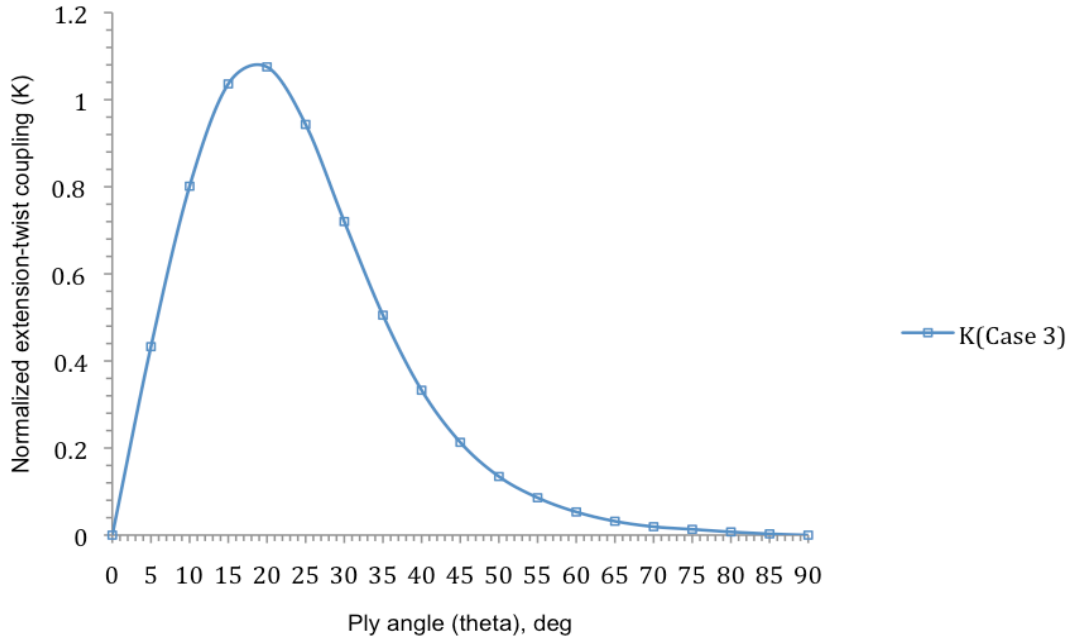


Figure 4.9 Normalized extension-twist coupling (K) as a function of ply Angle (Case 3)

#### 4.1.4 Case-4: $E_{22} = 1/100^{th}$ of Composite

Elastomer stiffness is assumed to be lowered two orders of magnitude in this case. Plots demonstrating the mechanical response of stiffnesses and extension-twist coupling display a similar behavior as in the previous case. The representation of axial stiffness plot (Figure 4.10) indicates that the level of axial stiffness is preserved in the cross-sectional configuration when compared to the stiffness plot from case 1. A normalized stiffness value of 1 and 0.057 are obtained for  $0^\circ$  and  $90^\circ$  composite ply lay-ups. Fundamentally the mechanical response of axial stiffness with a step increase in ply angle corresponds to the variation in  $Q_{11}$  term of the reduced stiffness matrix derived from classical composite lamination theory.

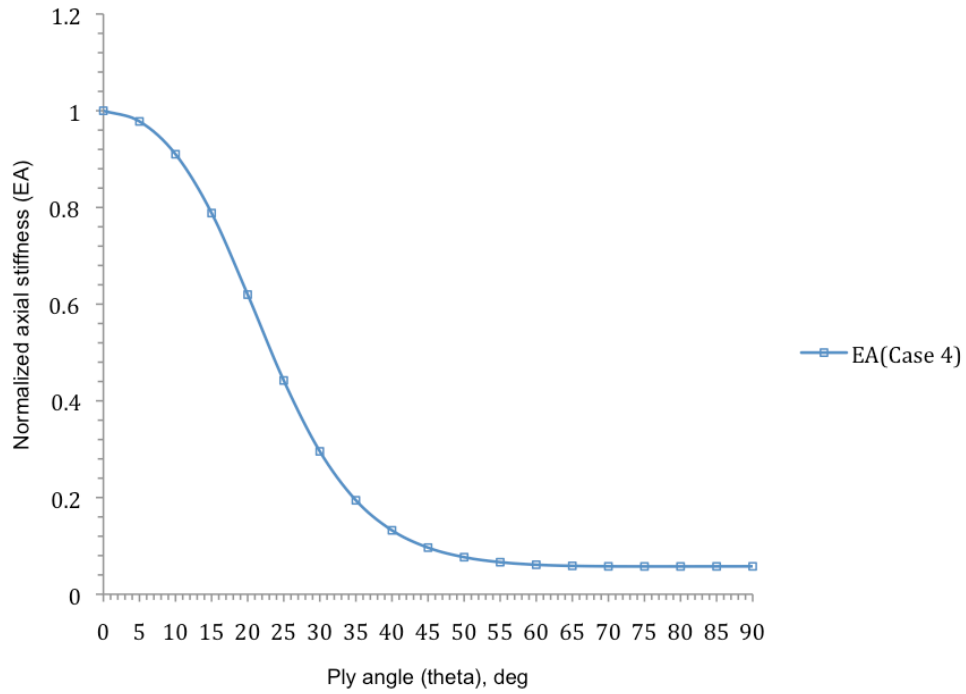


Figure 4.4 Normalized axial stiffness (EA) as a function of ply angle (Case 4)

Figures 4.5 and 4.6 represent the normalized torsional stiffness and extension-twist coupling as a function of ply angle for a constant value of elastomeric stiffness and Poisson's ratio. Although a symmetric mechanical behavior still persists for the trend in torsional stiffness, a significant reduction is observed at the beginning with decrease in elastomer stiffness. Normalized torsional stiffness values corresponding to  $0^\circ$  and  $90^\circ$  ply lay-ups is  $2.324 \times 10^3$ . For a  $45^\circ$  ply set-up, torsional stiffness is shown to be highest with a value of  $2.770 \times 10^3$ .

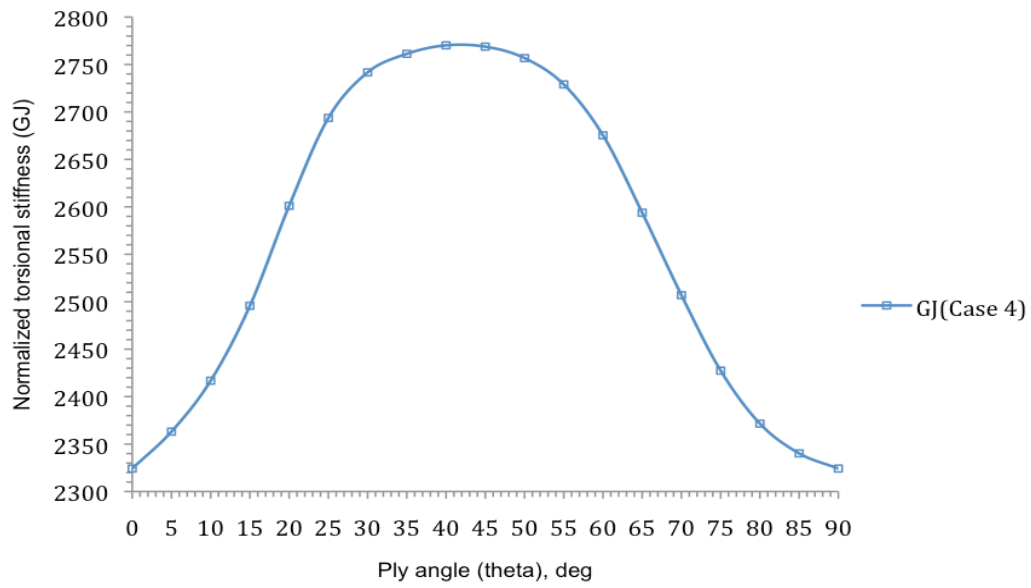


Figure 4.5 Normalized torsional stiffness ( $GJ$ ) as a function of ply angle (Case 4)

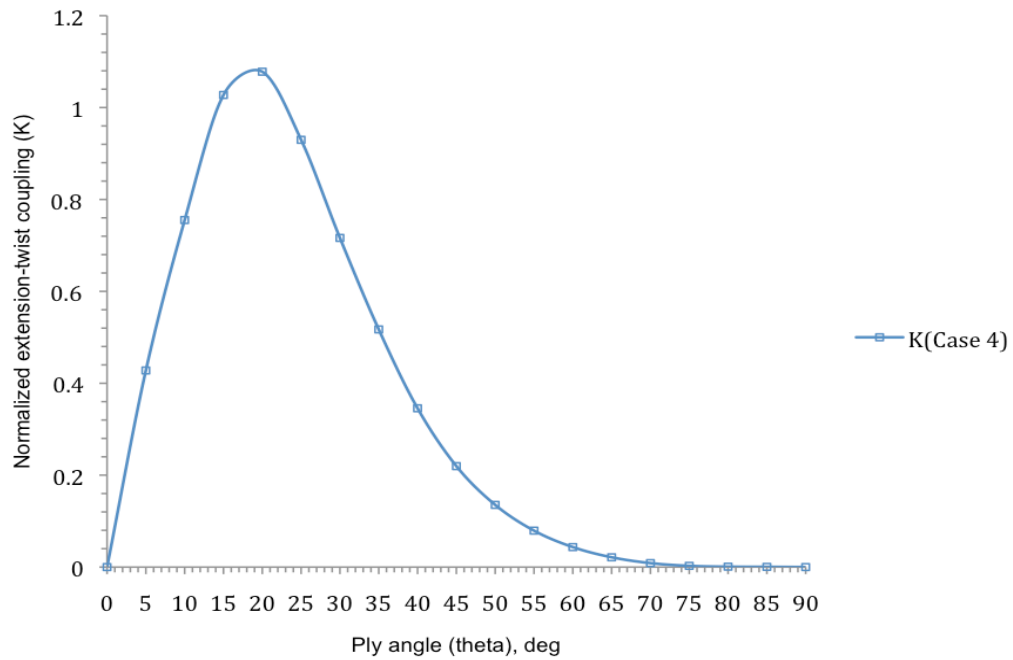


Figure 4.6 Normalized extension-twist coupling ( $K$ ) as a function of ply angle (Case 4)

Fundamentally a step-down in elastomer stiffness should represent a small improvement in the level of extension-twist coupling and it is shown in figure 4.6 that this concept holds true. Insignificant contributions towards the level of extension-twist coupling of the cross section is observed for  $0^\circ$  and  $90^\circ$  composite ply lay-ups by the presence and stiffness of the elastomeric strips.

#### 4.1.5 Case-5: Elastomeric Stiffness= $1/1000^{th} \times E_{22}$ of Composite

Reduction in elastomer stiffness to a value of 8.472 MPa causes the behavior of the torsionally compliant integral blade tip configuration to be similar to that of an open celled blade configuration. Figure 4.7 represents the axial stiffness plot as a function of ply angle and is shown that the effect of elastomer stiffness is invariant to the level of axial stiffness exhibited by the integral blade tip configuration. Normalized stiffness value corresponding to  $0^\circ$  and  $90^\circ$  ply angle is 1 and 0.057 respectively.

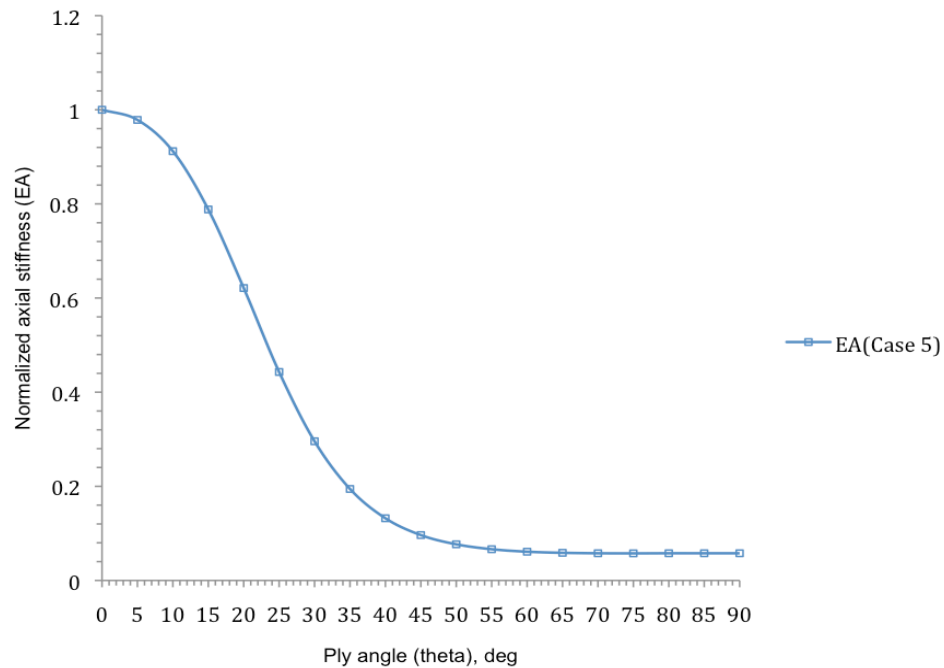


Figure 4.7 Normalized axial stiffness (EA) as a function of ply angle (Case 5)

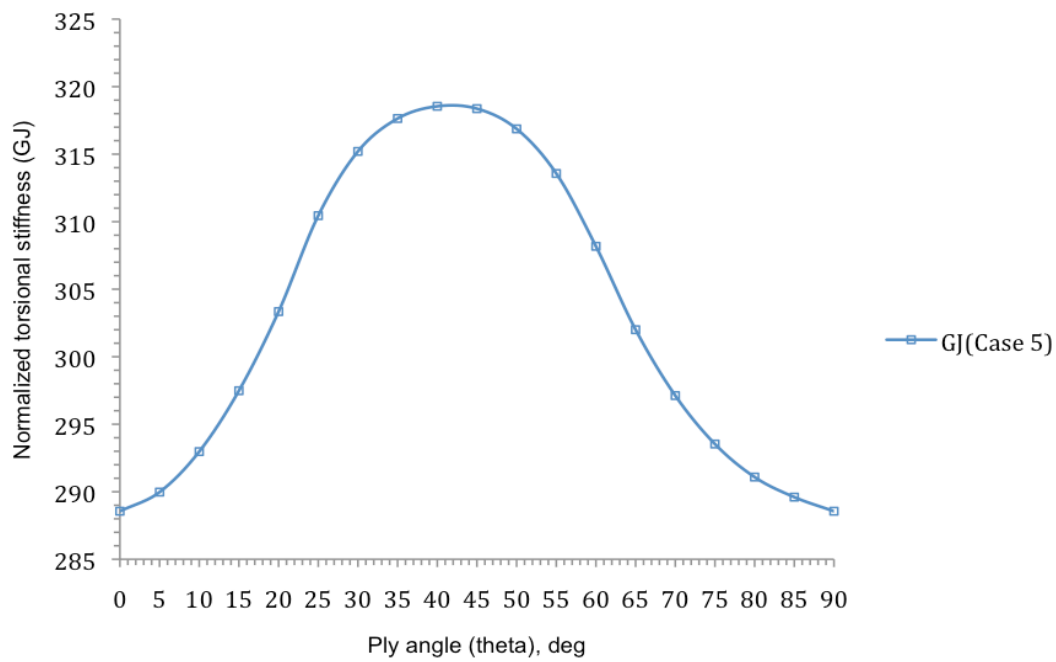


Figure 4.8 Normalized torsional stiffness (GJ) as a function of ply angle (Case 5)

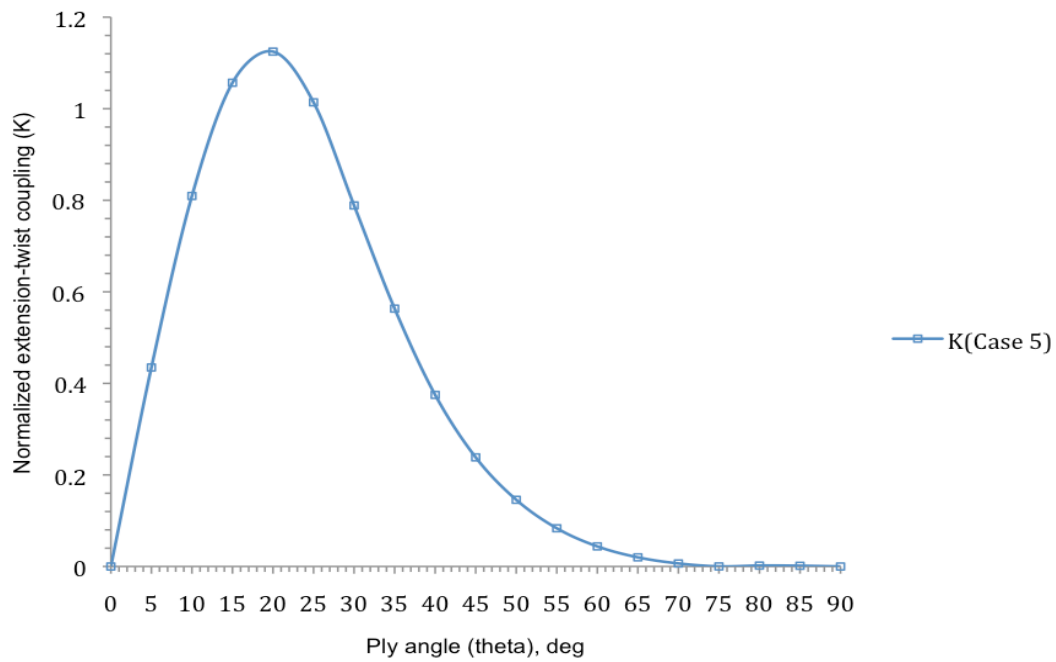


Figure 4.9 Normalized extension-twist coupling (K) as a function of ply angle (Case 5)



Maximum normalized value attained by extension-twist coupling for a 20° composite ply lay-up is 1.124 (Figure 4.9).

#### 4.1.6 Combined Normalized Stiffness and Extension-Twist Coupling Plots

Combined normalized plots of axial stiffnesses, torsional stiffnesses and the extension-twist coupling as a function of ply angle are shown in Figures 4.10, 4.11 and 4.12 for each of the cases when the elastomer stiffness is 0.1, 0.01, and 0.001 of the graphite/epoxy transverse axial stiffness, respectively. For the case of axial stiffness, little variation is seen with varying elastomer stiffness. This is expected because its stiffness and cross sectional area is negligible compared to that of the composite. A similar trend is seen for extension-twist coupling, which agrees with expectations since the coupling is caused by the asymmetric layup in the laminate. A slight increase is seen for lower values of the elastomer stiffness.

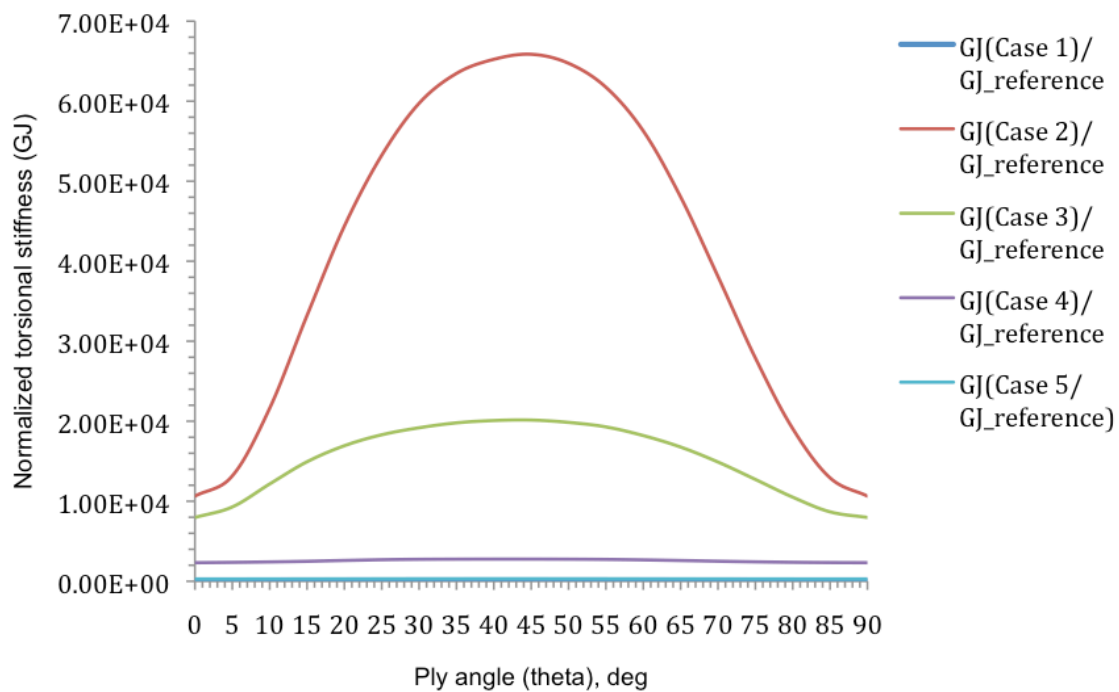


Figure 4.10 Combined normalized torsional stiffnesses (GJ) as a function of ply angle

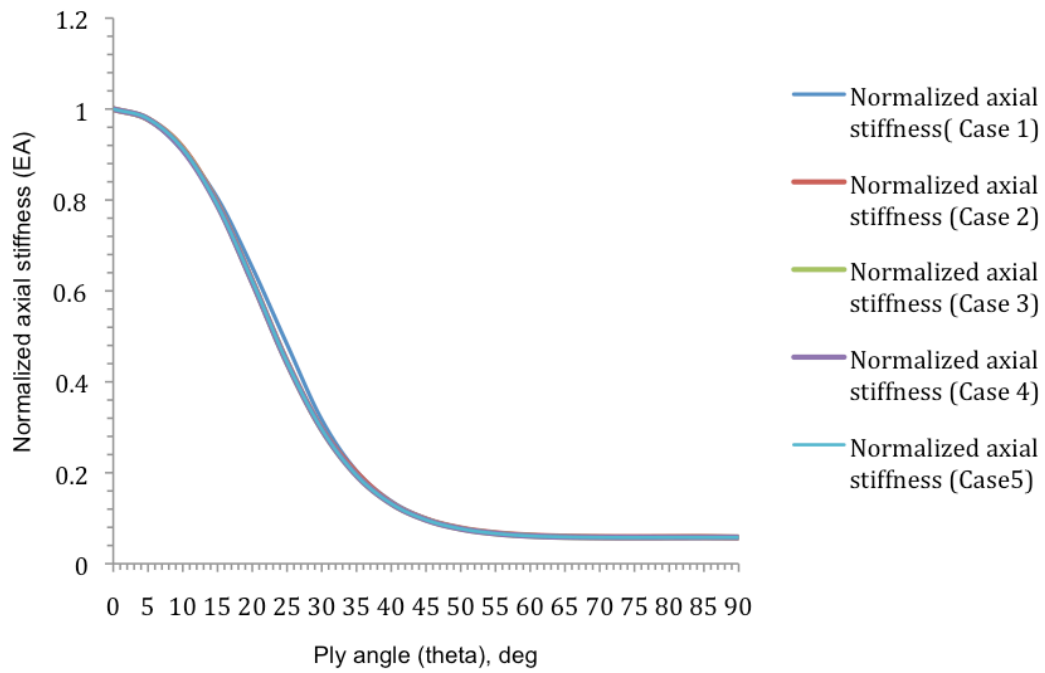


Figure 4.11 Combined normalized axial stiffnesses (EA) as a function of ply angle

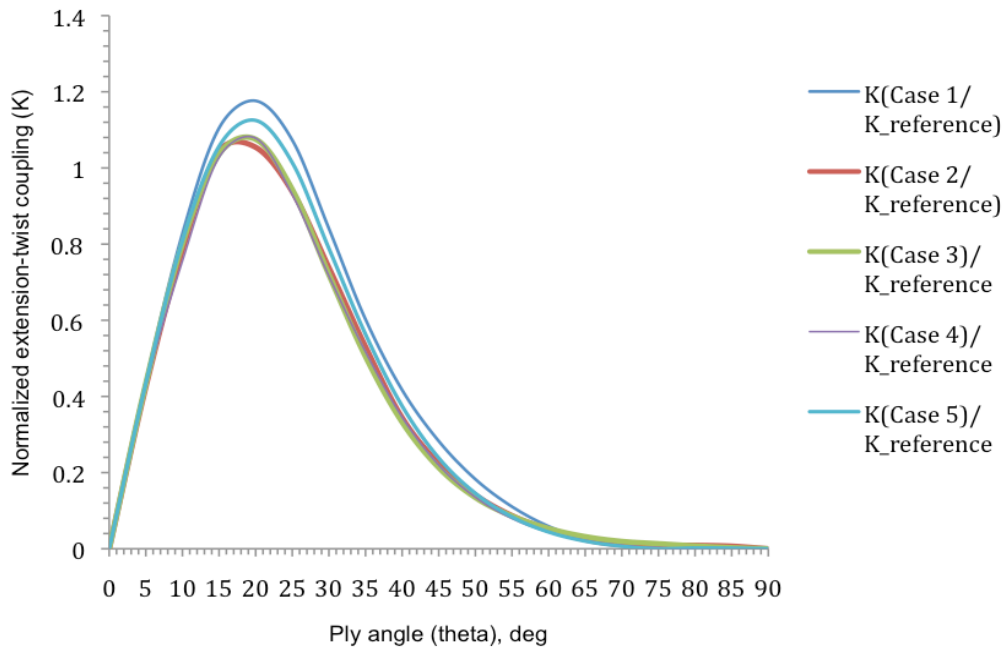


Figure 4.12 Combined normalized extension-twist coupling (K) as a function of ply angle

Based upon the results of this initial investigation it is observed that maximum amount of torsional compliance is exhibited by the open-celled blade structure configuration without elastomeric strips and the maximum level of torsional stiffness is generated by the configuration including elastomeric strips with an elastic modulus equal to the transverse stiffness of the composite laminate. It is also equally interesting to note that the torsional stiffness is very sensitive to changes in elastomer stiffness and ply angle (Case 3 vs. Case 4 vs. Case 5). Fundamentally this also demonstrates the fact that the proposed integral blade tip configuration tends to behave more like an open-cell cross-sectional configuration for small stiffness numbers assigned to elastomer strips. The maximum level of extension-twist coupling is generated for a ply lay-up between  $20^\circ$  and  $25^\circ$  for all the cases investigated.

As expected, Figure 4.11 and Figure 4.13 shows that the three axial stiffness curves collapse onto each other. It also shows that the axial stiffness of the cross section is not significantly influenced by the presence and the stiffness of the elastomeric strips, given their small cross-sectional area. It is interesting to note from Figure 4.10 and Figure 4.15, that the torsional stiffness shows a significant variation with elastomer stiffness (Case 3 vs. Case 4 vs. Case 5), while at the same time the level of extension-twist coupling (Figure 4.12 and Figure 4.14) shows only a small variation.

## CHAPTER 5

### CONCLUSIONS AND RECOMMENDATIONS FOR FUTURE WORK

A novel bi-material extension-twist coupled torsionally compliant star-beam type integral blade tip configuration for rotorcraft applications is proposed, modeled and parametrically investigated. The blade-tip structure is characterized by the incorporation of a set of isotropic, homogeneous, thin walled elastomer strips on the top and bottom surfaces of the open star configuration thus generating a quasi-closed cross-sectional configuration. The model is investigated through parametric variations in elastomeric stiffness. The parameters assumed in this work are the ply orientation angle and stiffness of elastomeric strips.

Torsional stiffness in particular, was found to be very sensitive to elastomer strip stiffness (Figure 4.12), which follows from a consideration that with increased elastomer stiffness, the structure tends away from an open-section in favor of a closed cross-sectional configuration.

Based upon the results of this initial finite element investigation it therefore appears that the use of elastomeric strips to bridge the gaps between the composite strips of the cross-section as the one in Figure 3.2 provides a window to increase the level of torsional stiffness without any significant decrease in axial stiffness or level of extension-twist coupling. The stiffness of the elastomeric strip is an effective parameter governing this response. Thus the variation of torsional stiffness and extension-twist coupling associated with each case study illustrates the tailoring characteristics of this novel bi-material integral blade tip configuration.

This initial finite element investigation confirmed that the use of elastomeric strips to bridge the gaps between the strips of an extension-twist coupled generalized star-beam airfoil cross section provides an effective means to increase the torsional stiffness of the cross-section without sacrificing the level of extension-twist coupling.

These initial results provide motivation to perform a more in-depth investigation to analyze the full capability of the concept. The research initiated in this thesis points to several other new and equally interesting areas of inquiry. The recommended research areas for future work are:

1. The development of an analytical model for the integral blade-tip configuration to enable parametric studies where a large number of candidate configurations need to be evaluated quickly and economically.
2. The dynamic response of an extension-twist coupled integral blade-tip configuration to isolate aeroelastic effects and stability.
3. The definition, development and investigation of optimum actuation requirements to augment the passive elastically tailored extension-twist coupling.
4. The fatigue behavior of extension-twist coupled bi-material airfoil shape composite star-beams, which are pertinent to rotorcraft and wind turbine applications.
5. The mechanical response investigation of blade tip structure developed from a cambered airfoil or other wind turbine specific airfoil designs.
6. The mechanical behavior study of torsionally compliant blade tip structure subjected to several other parameters that can be varied; e.g. elastomer strip thickness, Poisson's ratio, localized variation in elastomer stiffness and thickness, applied concentrated force and torque, the total number of elements, element type, material system and variable spatial distribution of rubber strips along and across the blade tip contour.
7. The determination of key parameters that play an influential role towards the achievement of optimum level of extensional-twist coupling.

8. The investigation of an optimal composite layup that provides the best level of extension-twist coupling.
9. The examination of mechanical response of the torsionally compliant blade tip structure in terms of center of mass and in terms of center of shear.
10. The development of a pitch controllable torsionally compliant mechanism specifically for wind turbine applications.
11. The study of the effect of elastomer strips on axial stiffness, torsional stiffness and level of extension-twist coupling for a integral blade tip associated with a hygrothermally stable composite stacking sequence and to a set of ‘Winckler’ composite stacking sequence series [5].
12. The mechanical behavior study of the integral blade tip subjected to a uniformly increasing centrifugal field.
13. The comprehensive investigations of flexural rigidity of the integral blade tip in response to a variation in several parameters.

## REFERENCES

- [1] Dancila, D. S., Kim, I.B. and Armanios, E. A., "Star-Shape Cross Section-Extension-Twist-Coupled Composite Beams for Rotorcraft Applications " *Proceedings of 54<sup>th</sup> AHS Annual Forum and Technology Display, American Helicopter Society Inc*, pp 1044-1049.
- [2] Kim, I., Dancila, D. S., Armanios, E. A., "Design, Manufacturing and Testing of Elastically Tailored Composite Star-beam Configurations," *Proceedings of the 44<sup>th</sup> AIAA/ASME/ASCE/AHS/ASC Structures, Structural Dynamics, and Materials Conference*, Norfolk, VA, 7-10 April 2003, pp. 4275-4283. AIAA Paper 2003-1866.
- [3] Dancila, D. S., Kim, I. B., and Armanios, E. A., "Efficient Implementation of Extension-Twist Coupling for Rotorcraft Applications *Proceedings of AHS Technical Specialists Meeting on Affordable Composite Structures*, Bridgeport, Connecticut, October 7-8, 1998.
- [4] Dancila, D. S., Kim, I. B., "Characterization of Modified Star Shape Cross-Sectional Beam Configurations with Rotorcraft Applications," *Proceedings of the 44<sup>th</sup> AIAA/ASME/ASCE/AAHS/ASC Structures, Structural dynamics, and Materials Conference*, Norfolk, VA, 7-10 April 2003.
- [5] Winckler, S. I., "Hygrothermally Curvature Stable Laminates with Tension-Torsion Coupling," *Journal of the American Helicopter Society*, Vol. 31, No.7, July 1985, pp. 56-58.

[6] ABAQUS v6.10 CAE Users Manual.



## BIOGRAPHICAL INFORMATION

Sthanu Mahadev was born in Chennai, India on December 7, 1987. He received his Bachelor of Science degree in Aeronautical Engineering from Anna University (India) in 2004. He was the proud recipient of “ Central Reserve Police Force Defense Personnel’s Meritorious Student” scholarship through out his under graduate career.

His undergraduate research work topic was “Design and Analysis of Control Surfaces of a Typical Regional Transport Aircraft Using CAD/CAE Tools”. After graduating in 2008 with honors, he was immediately absorbed as a software design engineer in the multinational software company Tata Consultancy Services and gained broad experience in a multitude of aerospace design softwares. He subsequently was admitted to the graduate program in the Mechanical and Aerospace Engineering Department at The University of Texas at Arlington. He is also a distinguished student member of the prestigious engineering honor society Phi Kappa Phi since June 2009 and the well-revered aeronautics and astronautics society AIAA since January 2010.